The Mid-Infrared Properties of Blue Compact Dwarf Galaxies

Yanling Wu¹, V. Charmandaris^{2,3}, J.R. Houck¹, J. Bernard-Salas¹, V. Lebouteiller¹

ABSTRACT

The unprecedented sensitivity of the Spitzer Space Telescope has enabled us for the first time to detect a large sample of Blue Compact Dwarf galaxies (BCDs), which are intrinsically faint in the infrared. In the present paper we present a summary of our findings which providing essential information on the presence/absence of the Polycyclic Aromatic Hydrocarbon features in metal-poor environments. In addition, using Spitzer/IRS high-resolution spectroscopy, we study the elemental abundances of neon and sulfur in BCDs and compare with the results from optical studies. Finally, we present an analysis of the mid- and far-infrared to radio correlation in low luminosity low metallicity galaxies.

Subject headings: galaxies: ISM — infrared: galaxies — infrared: ISM — ISM: dust, extinction — ISM: structure

1. Introduction

Blue compact dwarf galaxies (BCDs) are dwarf galaxies with blue optical colors resulting from one or more intense bursts of star formation, low luminosities ($M_B > -18$), and small sizes. Although BCDs are defined mostly by their morphological parameters, they are globally found to have low heavy element abundances as measured from their HII regions $(1/30 - 1/2 Z_{\odot})$, Izotov & Thuan, 1999). The low metallicity of BCDs is suggestive of a young age, since their interstellar medium is chemically unevolved. However, some low metallicity BCDs (i.e. IZw18) do display an older stellar population and have formed a large fraction of their stars more than 1 Gyr ago (see Aloisi et al. 2007). The plausible scenario that BCDs are young is intriguing within the context of cold dark matter models which predict

¹Astronomy Department, Cornell University, Ithaca, NY 14853

²University of Crete, Department of Physics, Heraklion, GR-71003, Greece

³IESL/FORTH, Heraklion, GR-71110, Greece, & Chercheur Associé, Obs. de Paris, F-75014, France

that low-mass dwarf galaxies, originating from density perturbations much less massive than those producing the larger structures, can still be forming at the current epoch. However, despite the great success in detecting galaxies at high redshift over the past few years, bona fide young galaxies still remain extremely difficult to find in the local universe (Kunth & Östlin 2000). This is likely due to the observational bias of sampling mostly luminous, more evolved galaxies at high redshifts. If some BCDs are truly young galaxies, they would provide an ideal local laboratory to understand the galaxy formation processes in the early universe.

Accumulated observational evidence over the recent years provided more details on the unique properties of these galaxies (for a review see Kunth & Östlin 2000). Early ground-based observations by Roche et al. (1991) on the MIR spectra of 60 galaxies revealed that Polycyclic Aromatic Hydrocarbon (PAH) emission is generally suppressed in low-metallicity galaxies, which could be due to hard photons destroying the particles that produce the unidentified infrared bands. The suppression of the PAH emission is also seen in the mid-IR spectra of four BCDs discussed by Madden (2000), Galliano et al. (2005), and Madden et al. (2006). More recent work based on *Spitzer* observations has confirmed that PAH emission is missing in the most metal-poor galaxies (Houck et al. 2004b; Engelbracht et al. 2005,2008; Wu et al. 2006, 2007a; Rosenberg et al. 2006). Dwek (2005) proposed that the delayed injection of carbon molecules into the interstellar medium (ISM) might be partly responsible for the absence of PAH features in young star-forming regions, or for the existence of a metallicity threshold below which PAHs have not formed.

For our study, as part of the IRS (Houck et al. 2004a) Guaranteed Time Observation (GTO) program, we have compiled a large sample (\sim 60) of BCD candidates selected from the Second Byurakan Survey (SBS), Bootes void galaxies, and other commonly studied BCDs. We obtained low-resolution and high-resolution 5-35 μ m spectra, as well as 16 and 22 μ m peak-up images for our sample. Full details on our observation strategy and data reduction as well as ancillary data used can be found in Wu et al. (2006,2007a, 2007b,2008).

2. Results

The 5-38 μ m low-resolution spectra for 12 BCDs were published by Wu et al. (2006) where we refer the reader for their detailed description. In brief, the mid-IR spectra of these low-metallicity galaxies display a variety of spectral features. PAH emission is absent in some BCDs, such as IZw18 and SBS0335-052, while prominent PAH emission was detected in other BCDs, including NGC1140. Fine structure lines of [SIV]10.51 μ m, [NeII] 12.81 μ m, [NeIII] 15.55 μ m and [SIII] 18.71 μ m were detected in most BCDs even from the low-resolution spectra and line flux measurements for 13 BCDs from the high-resolution data can be found in Wu et al. (2008).

2.1. PAH emission in low metallicity galaxies

As mentioned earlier the absence of PAH emission could be due to the low abundance of carbon and/or nucleating grains. To examine a possible variation in the PAH EW with metallicity, we plot the PAH Equivalent Widths (EWs) of 6.2 and $11.2 \,\mu m$ for our sample as a function of their metallicities. We can see that PAH emission is absent in the most metal-poor BCDs and it appears that there is a trend showing that galaxies with a lower metallicity may have smaller PAH EWs (see Fig. 7 in Wu et al. 2006).

The presence of a young starburst in a low-metallicity environment results in the production of high-energy photons that can propagate relatively large distances before being absorbed by the metals in the ISM. Because of the rather large difference in the ionization potentials of Ne⁺⁺ (41 eV) and Ne⁺ (22 eV), the ratio of [NeIII]/[NeII] is a good tracer of the hardness of the interstellar radiation field. We observe that the PAH EWs at 6.2 and 11.2 μ m are generally suppressed in a harder radiation field as indicated by a larger [NeIII]/[NeII] ratio, suggesting that the deficiency in PAH emission may be related to the destruction of the photodissociation region (PDR) by hard UV photons. Another important parameter of the radiation field is its UV luminosity density. In young starbursts, L_{FIR} is representative of the total UV luminosity. We plot the PAH EWs as a function of its 22 μ m luminosity density and find that there is a trend that PAH EW decreases with increasing luminosity density. However, there is large scatter to both relations.

We have shown that there are generally weaker PAHs in metal-poor environments. We have also discussed the effects of the hardness of the radiation field and the luminosity density on the destruction of PAH molecules. Is the absence of PAHs in metal-poor galaxies solely due to formation effects, destruction effects, or some combination? To examine this, we plot the PAH EW as a function of a new quantity: ([NeIII/[NeII])($L_{22\mu m}/V$)(1/Z), where the product of the neon ratio and the luminosity density represents the destruction effect and Z, the metallicity of the galaxy, represents the formation effect. We find that there is a much tighter anti-correlation (Fig. 1) as compared to other relations with PAHs that we have inspected on a series of parameters. This suggests that the absence of PAHs in a metal-poor environment is due to a combination of formation effects and destruction effects. A more detailed analysis on the variation of the various PAH bands on different environments over a large range on metallicities can be found on (Smith et al. 2007, Engelbracht et al 2008, and Galliano et al. 2008)

2.2. Elemental Abundances

Using the infrared fine structure lines, one can estimate the elemental abundances for some elements, i.e. neon and sulfur. There are several methods to derive the chemical abundances. We use an empirical method, which derives ionic abundances directly from the observed lines of the relavent ions. To do so, we need to have the flux of one hydrogen recombination line, the dust extinction, as well as the electron temperature and density of the interstellar medium (ISM).

In the wavelength range observed by the IRS, the flux of Hu α (12.37 μ m) line is most commonly used (converted to H β) to estimate the flux of ionized hydrogen. However, this line is usually faint in BCDs and in cases where Hu α is not detected, we use the radio continuum or H α images to derive the flux of H β . Since the infrared determination of elemental abundances does not depend strongly on the electron temperatures and densities, we adopt optically derived T_e and N_e from the literature. For sources where such information is not available, we assume a typical T_e of 10,000 K and N_e of 100 cm⁻³. We also adopted the E_{B-V} values calculated from hydrogen recombination lines from optical spectra for dust extinction, and in cases where there is strong evidence for dust-enshrouded regions, we estimate its dust extinction from the strength of silicate absorption features at 9.7 μ m.

In Figure 2 we plot the abundances of neon and sulfur for our BCD sample as derived from the IRS high-resolution data. Verma et al. (2003) have found a positive correlation between the neon and argon abundances for their sample of starburst galaxies using ISO observations, while their data show no correlation between the sulfur and neon and/or argon abundances (indicated as stars on Fig. 2). However, our sources show that the neon and sulfur abundances scale with each other. In the same figure, we also plot the proportionality line of the ratio for (Ne/S). The maximum and minimum values of the solar neon and sulfur abundances are indicated by the width of the gray band, and we find that most of our BCDs have ratios above those values, indicating a higher Ne/S ratio than that has been found in the solar neighborhood. If we compare the infrared derived Ne/S ratios for BCDs with the optical derived Ne/S ratios, we find a discrepancy of a factor of \sim 2 (see Fig. 6 in Wu et al. 2008). This is probably due to the difference in the infrared and optical methods for estimating elemental abundances (e.g. the uncertainties in the ICFs adopted by optical studies). However, the average Ne/S ratio of the 13 BCDs we studied (12.5 \pm 3.1) is consistent with the Ne/S ratios derived in the HII regions from several other studies.

2.3. The Infrared/Radio Correlation

The FIR/radio correlation is known to be ubiquitous among many late type galaxies. However, little could be done for low luminosity systems. Hopkins et al. (2002) found that the star formation rates (SFRs) estimated from 1.4 GHz and $60 \,\mu$ m luminosities agree with each other for the BCDs they studied, while Wu et al. (2005) indicated a slope change for dwarf galaxies in a similar comparison of SFRs. A number of deep Spitzer mid-IR and FIR

surveys can now probe a population of galaxies with low infrared luminosities, for which ancillary data, including deep radio imaging, are becoming available. With these new data, we will be able to investigate the connection between the infrared and radio emission in low luminosity systems.

In Fig. 1 of Wu et al. (2007b), we plot the radio luminosity of our sample as a function of the FIR luminosity. The luminosities of the sources we study span nearly 4 orders of magnitudes, but the correlation between the FIR and the radio is remarkably tight with a scatter less that a factor of 2 and consistent with a linear fit of with slope $q_{FIR}=1.09\pm0.07$ which agrees well with the slope of 1.10 ± 0.04 found by Bell (2003) for a sample of 162 galaxies, as well as the slope of 1.11 ± 0.02 for the infrared selected sources from the IRAS Bright Galaxy Sample (BGS) (Condon et al. 1991). Using the MIPS $24\mu m$ data we also examined the MIR to radio correlation for our sample following the definition of q_{24} by Appleton et al. (2004). We find that $q_{24}=1.3\pm0.4$, slightly higher than the average q_{24} for the galaxies in the first look survey (Appleton et al. 2004), though still consistent within 2σ (see Fig. 2 of Wu et al. 2007b. We search for correlations between the q ratios of the galaxies in our sample with a few physical parameters, such as metallicity, dust temperature, etc. We do not see any clear correlation between the q ratios and the temperature, while for the metallicity of our sample, we find that q_{24} is generally suppressed for metal-poor sources $(12+\log(O/H)<8.0)$, with SBS0335-052E as a clear outlier (see Fig. 3). A more detailed discussion on the q_{24} ratio with metallicity can be found in Wu et al. (2007b).

3. Summary

We have explored the mid-IR properties of BCDs with the Spitzer Space Telescope. Using the low-resolution and high-resolution modules of the IRS, we have obtained 5-35 μ m spectra for our BCD sample. PAH emission at 6.2, 7.7, 11.2 and 12.8 μ m is detected in some BCDs, though their strength varies substantially, and we find that the suppression of PAHs in metal-poor harsh environment is likely due to a combination of formation and destruction effects. Using infrared fine-structure lines, we have also estimated the elemental abundances of neon and sulfur for 13 BCDs. It appears Ne and S abundances are well correlated in our sample, while their ratio is higher than the values found in the solar neighborhood. The infrared derived Ne/S ratio is also a factor of 2 higher than the optical derived Ne/S ratio for the same sample, though our result is consistent with the Ne/S found by other infrared studies in HII regions. Finally, we have also investigated the IR/radio correlation in low luminosity systems and we find that both the mid-IR and FIR luminosities scale with the radio luminosities, though the scatter is larger for mid-IR/radio.

REFERENCES

Aloisi, A., et al. 2007, ApJ, 667, L151

Appleton, P. N., et al. 2004, ApJS, 154, 147

Bell, E. F. 2003, ApJ, 586, 794

Brandl, B. R., et al. 2006, ApJ, 653, 1129

Condon, J. J., Anderson, M. L., & Helou, G. 1991, ApJ, 376, 95

Dwek, E. 2005, The SEDs of Gas-Rich Galaxies: Confronting Models with Data, 761, 103

Engelbracht, C. W., et al. 2005, ApJ, 628,L29

Engelbracht, C. W., et al. 2008, ArXiv e-prints, 801, arXiv:0801.1700

Galliano, F., et al. 2005, A&A, 434, 867

Galliano, F., et al. 2008, ArXiv e-prints, 801, arXiv:0801.4955

Helou, G., Soifer, B. T., & Rowan-Robinson, M. 1985, ApJ, 298, L7

Hopkins, A. M., Schulte-Ladbeck, R. E., & Drozdovsky, I. O. 2002, AJ, 124, 862

Houck, J. R., et al. 2004a, ApJS, 154, 18

Houck, J. R., et al. 2004b, ApJS, 154, 211

Izotov, Y. I., & Thuan, T. X. 1999, ApJ, 511, 639

Kunth, D. & Östlin, G. 2000, A&A Rev., 10, 1

Madden, S. C., Galliano, F., Jones, A. P., & Sauvage, M. 2006, A&A, 446, 877

Madden, S. C. 2000, New Astronomy Review, 44, 249

Roche, P. F., Aitken, D. K., Smith, C. H., & Ward, M. J. 1991, MNRAS, 248, 606

Rosenberg, J. L., Ashby, M. L. N., Salzer, J. J., & Huang, J.-S. 2006, ApJ, 636, 742

Smith, J. D. T., et al. 2007, ApJ, 656, 770

Verma, A., et al. 2003, A&A, 403, 829

Wu, H., et al. 2005, ApJ, 632, L79

Wu, Y., et al. 2006, ApJ, 639, 157

Wu, Y., et al. 2007a, ApJ, 662, 952

Wu, Y., et al. 2007b, ArXiv e-prints, 711, arXiv:0711.4363

Wu, Y., et al. 2008, ApJ, 673, 193

This preprint was prepared with the AAS IATEX macros v5.2.

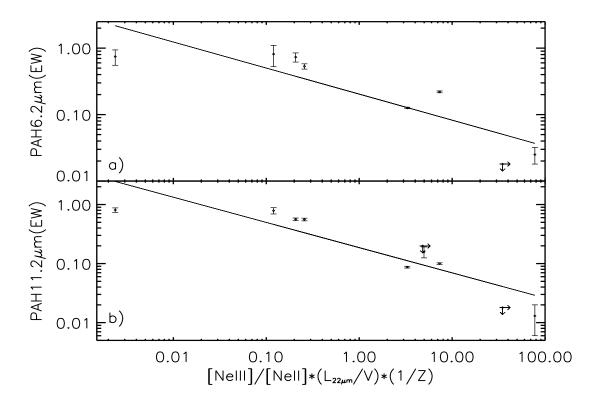


Fig. 1.— a) The PAH EW at $6.2\,\mu\mathrm{m}$ vs the product of the hardness of the radiation field and the luminosity density, divided by the metallicity of the galaxy. We can see that there is an anti-correlation that the PAH EW decreases when the factor ([NeIII]/[NeII])×(L_{22 $\mu\mathrm{m}$}/V)×(1/Z) increases. b) Same as a) but for the 11.2 $\mu\mathrm{m}$ PAH (see section 4.6 in Wu et al. 2006 for more details).

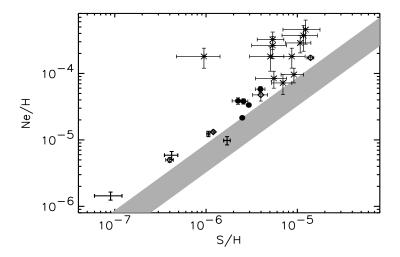


Fig. 2.— A plot of the Ne/H vs S/H abundance. Our BCDs are indicated by the filled circles if $\operatorname{Hu}\alpha$ is detected and by diamonds if it is not detected. The sources that are shown by only the error bars are those that have non-detection of [NeII] or [SIII]. The starburst galaxies from Verma et al. (2003) are marked with the stars. We use the grey band to indicate the locus on the plot where the ratio of Ne/S would be consistent with the different solar values for neon and sulfur abundances (see section 4.2 in Wu et al. 2008 for more details).

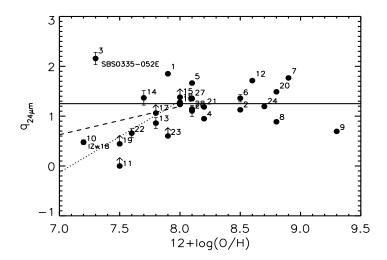


Fig. 3.— The q_{24} ratio plotted as a function of the oxygen abundance of the BCDs. The mean q_{24} value for all the sources is indicated by the solid line. A fit to the low metallicity sources $(12+\log(O/H)\leq 8.0)$ is indicated by the dashed line; while the dotted line is the same fit excluding SBS0335-052E (see section 3.2 in Wu et al. (2007b) for more details).